PLOS GENETICS

RESEARCH ARTICLE

Biology and engineering of integrative and conjugative elements: Construction and analyses of hybrid ICEs reveal element functions that affect species-specific efficiencies

Emily L. Bean, Calvin Herman, Mary E. Anderson, Alan D. Grossman*

Department of Biology, Massachusetts Institute of Technology, Cambridge, Massachusetts, United States of America

* adg@mit.edu

OPEN ACCESS

Citation: Bean EL, Herman C, Anderson ME, Grossman AD (2022) Biology and engineering of integrative and conjugative elements: Construction and analyses of hybrid ICEs reveal element functions that affect species-specific efficiencies. PLoS Genet 18(5): e1009998. https://doi.org/10.1371/journal.pgen.1009998

Editor: Daniel B. Kearns, Indiana University, UNITED STATES

Received: December 16, 2021

Accepted: April 4, 2022

Published: May 18, 2022

Data Availability Statement: All relevant data are within the manuscript and its Supporting Information files.

Funding: Research reported here is based upon work supported, in part, by the National Institute of General Medical Sciences of the National Institutes of Health (https://www.nigms.nih.gov/) under award number R35 GM122538 to ADG. The funders had no role in study design, data collection

Abstract

Integrative and conjugative elements (ICEs) are mobile genetic elements that reside in a bacterial host chromosome and are prominent drivers of bacterial evolution. They are also powerful tools for genetic analyses and engineering. Transfer of an ICE to a new host involves many steps, including excision from the chromosome, DNA processing and replication, transfer across the envelope of the donor and recipient, processing of the DNA, and eventual integration into the chromosome of the new host (now a stable transconjugant). Interactions between an ICE and its host throughout the life cycle likely influence the efficiencies of acquisition by new hosts. Here, we investigated how different functional modules of two ICEs, Tn*916* and ICE*Bs1*, affect the transfer efficiencies into different host bacteria. We constructed hybrid elements that utilize the high-efficiency regulatory and excision modules of ICE*Bs1* and the conjugation genes of Tn*916*. These elements produced more transconjugants than Tn*916*, likely due to an increase in the number of cells expressing element genes and a corresponding increase in excision. We also found that several Tn*916* and ICE*Bs1* components can substitute for one another. Using *B. subtilis* donors and three *Enterococcus* species as recipients, we found that different hybrid elements were more readily acquired by some species than others, demonstrating species-specific interactions in steps of the ICE life cycle. This work demonstrates that hybrid elements utilizing the efficient regulatory functions of ICE*Bs1* can be built to enable efficient transfer into and engineering of a variety of other species.

Author summary

Horizontal gene transfer helps drive microbial evolution, enabling bacteria to rapidly acquire new genes and traits. Integrative and conjugative elements (ICEs) are mobile genetic elements that reside in a bacterial host chromosome and are prominent drivers of

and analysis, decision to publish, or preparation of the manuscript.

Competing interests: The authors have declared that no competing interests exist.

horizontal gene transfer. They are also powerful tools for genetic analyses and engineering. Some ICEs carry genes that confer obvious properties to host bacteria, including antibiotic resistances, symbiosis, and pathogenesis. When activated, an ICE-encoded machine is made that can transfer the element to other cells, where it then integrates into the chromosome of the new host. Specific ICEs transfer more effectively into some bacterial species compared to others, yet little is known about the determinants of the efficiencies and specificity of acquisition by different bacterial species. We made and utilized hybrid ICEs, composed of parts of two different elements, to investigate determinants of transfer efficiencies. Our findings demonstrate that there are species-specific interactions that help determine efficiencies of stable acquisition, and that this explains, in part, the efficiencies of different ICEs. These hybrid elements are also useful in genetic engineering and synthetic biology to move genes and pathways into different bacterial species with greater efficiencies than can be achieved with naturally occurring ICEs.

Introduction

Integrative and conjugative elements (ICEs), also called conjugative transposons, are mobile genetic elements that are major drivers of bacterial evolution [1–5]. They reside in a host chromosome and can transfer to a recipient cell in a contact-dependent process termed conjugation. ICEs often contain cargo genes that are not needed for the ICE life cycle, but that confer various phenotypes to host cells, including antibiotic resistances, pathogenicity, symbiosis, and various metabolic capabilities [3,6,7]. In addition to their natural functions, ICEs have been engineered to allow genetic manipulation of a range of organisms [8–10].

ICEs spend most of their time integrated in and passively propagated with the chromosome of the host cell. Either stochastically or in response to some signal(s), ICEs use element-encoded site-specific recombination machinery to excise from the chromosome to form a plasmid. At this stage, many (perhaps most or all) ICEs replicate autonomously by rolling-circle replication [2,11–14]. The element-encoded relaxase nicks and becomes covalently attached to the 5' end of DNA at the origin of transfer (*oriT*), and host-encoded replication machinery, including a helicase and DNA polymerase, is recruited for unwinding and replicating the ICE DNA [12–17]. For the two ICEs used here, Tn*916* and ICE*Bs1* (see below), autonomous replication is entirely independent of conjugation [12–14].

ICEs encode proteins that comprise the conjugation machinery, a type IV secretion system (T4SS) that transfers DNA from donor to recipient cells. In most cases, the DNA that is transferred is linear, single-stranded, and covalently attached to the relaxase [18–20]. Upon entry into the recipient, the linear ssDNA re-circularizes, becomes double-stranded following replication from a single-strand origin of replication (*sso*) [14,21], and eventually integrates into the chromosome of its new host to generate a stable transconjugant.

Although most ICEs follow the same general life cycle, they vary widely in the overall efficiency of transfer. Additionally, different ICEs have different natural host ranges: some ICEs are found in many different bacterial host species, whereas others have been found in only one species. In addition to their natural hosts, many ICEs can be transferred into species in which they are not naturally found [8–10,22,23].

The ability of ICE gene products to interact with host components at various steps of the ICE life cycle likely influences the efficiency or effectiveness of transfer out of and into different bacterial hosts. In particular, differences in efficiencies of activation, recombination (excision), DNA processing, unwinding and replication, the compatibility of the conjugation

machinery with donor and recipient cell wall and membrane structures, and the availability of a suitable integration site and the ability to integrate in nascent transconjugants could all impact the stable acquisition of an ICE [2,3,5].

We were interested in determining which step(s) of the ICE life cycle account for differences in conjugation efficiencies into various host species between two well-studied ICEs found in phylogenetically distinct cocci and rod-shaped Gram-positive organisms: Tn*916* (Fig 1A) and ICE*Bs1* (Fig 1B). In addition, because the natural hosts of these elements are different, we thought that insights into which parts of the life cycle led to different efficiencies could allow us to engineer elements with improved function in different hosts.

Tn*916* (~18 kb) was the first-discovered ICE and carries the tetracycline resistance gene *tetM* [24,25]. It and its close relatives are found in *Enterococcus*, *Streptococcus*, *Staphylococcus*, and *Clostridium* species [4,26–31]. Tn*916* is also functional in *Bacillus subtilis* {e.g., [14,32–34]} and other *Bacillus* species {e.g., [23,35]}.

ICE*Bs1* (~20.5 kb) of *B*. *subtilis* encodes conjugation and replication machinery homologous to that of Tn*916*. ICE*Bs1* has only naturally been observed in *B*. *subtilis*, although related sequences are found in several other *Bacillus* species [36,37]. ICE*Bs1* transfers into a variety of other *Bacillus* species (including *B*. *anthracis*, *B*. *cereus*, *B*. *thuringiensis*) and also a variety of *Enterococcus*, *Streptococcus*, and *Listeria* species [8,22,38].

Excision and transfer efficiencies of Tn*916* and ICE*Bs1* are affected by several different factors, making direct comparisons difficult. For example, excision frequencies of Tn*916* are different depending on the site of insertion and growth conditions, including the presence or absence of tetracycline [4,14,39–43]. Excision and transfer of ICE*Bs1* is affected by DNA damage, cell density, the identity of the neighboring cells, and growth conditions [22,44–46]. In order to compare efficiencies of DNA processing and conjugation functions of ICE*Bs1* to those of Tn*916*, we constructed and analyzed hybrid elements that contain the regulatory and integration-excision systems of ICE*Bs1* and the DNA processing and conjugation genes from Tn*916* or from ICE*Bs1*. We used these hybrid elements to analyze steps in the ICE life cycle that contribute to different conjugation efficiencies separate from excision and integration. We also used these hybrids to demonstrate the utility of such elements for genetic engineering as these hybrid elements can be acquired more efficiently by some recipient species than either parent element. The approaches described here are generalizable to many other elements and provide a platform for using the regulatory and integration-excision components of ICE*Bs1* for studying conjugation systems from other elements.

Results and discussion

Excision and conjugation efficiencies of ICE*Bs1* and Tn*916*

We compared the excision and conjugation efficiencies of Tn*916* and ICE*Bs1* in *B*. *subtilis* using typical mating conditions (on a filter on a solid substrate; Materials and Methods). The donor (host) strain with Tn*916* (CMJ253) has a single copy of the element integrated in the genome between *yufK* and *yufL* (see Materials and Methods). Tn*916* is regulated, at least in part, by a transcriptional attenuation mechanism that is partially relieved in the presence of tetracycline or other drugs that inhibit translation [4,39–43].

We used two different ICE*Bs1* donor strains. One donor (JMA384) contains essentially a wild type element with an antibiotic resistance gene (ICE*Bs1*::*kan*) for selection inserted between *yddM* and *attR* (Fig 1A) [22]. The second donor (JMA168) contains the deletion-insertion *Δ*(*rapI-phrI*)::*kan* and an inducible copy of the activator *rapI* (Pspank(hy)-*rapI*). Expression of *rapI* causes de-repression of ICE*Bs1* gene expression and subsequent excision, typically in 25–90% of the cells in a population [22,44,46]. We employed the inducible *rapI*

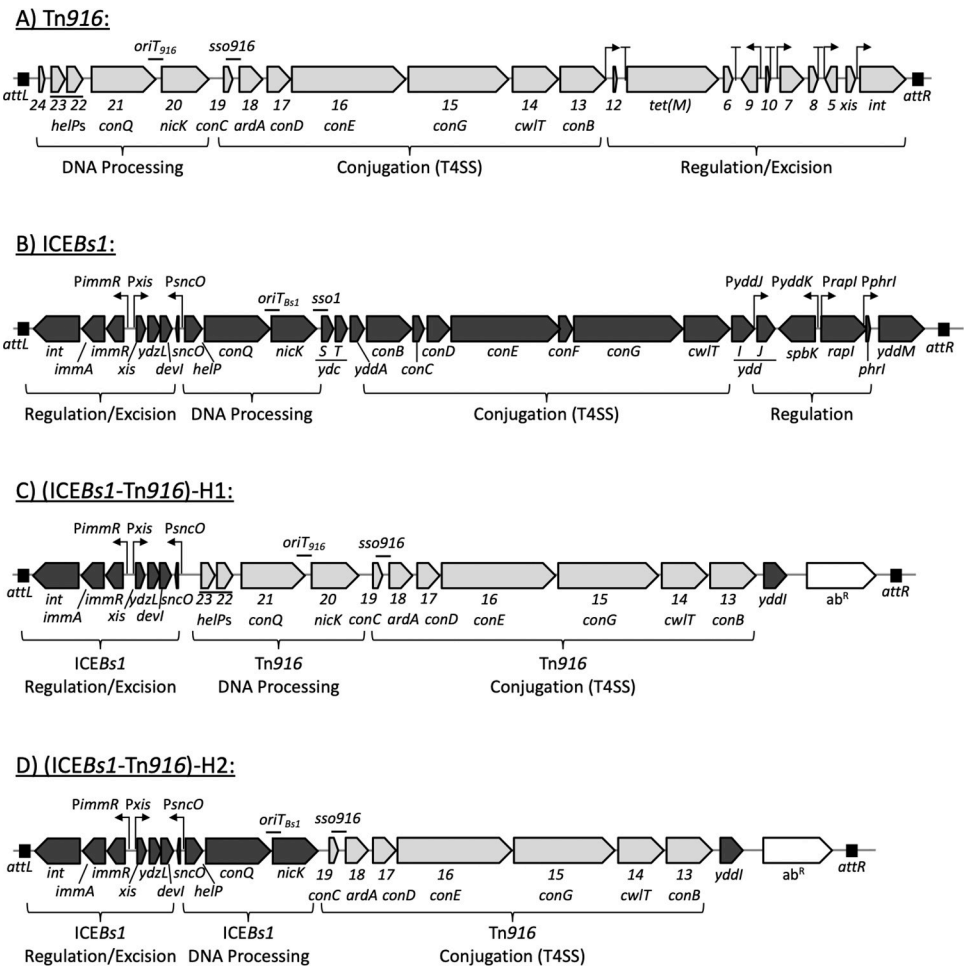

Fig 1. Genetic maps of ICE*Bs1*, Tn*916*, and hybrid elements. Maps are shown of the ICEs used in these experiments: A) Tn*916*; B) ICE*Bs1*; C) (ICE*Bs1*-Tn*916*)-H1 D) (ICE*Bs1*-Tn*916*)-H2. Attachment sites *attL* and *attR* are indicated by black boxes (ICE*Bs1*, (ICE*Bs1*-Tn*916*)-H1, and (ICE*Bs1*-Tn*916*)-H2 are all integrated at *trnS-leu2*; Tn*916* is integrated between *yufK* and *yufL* in donor cells. Open reading frames are indicated by horizontal arrows, pointing in the direction of transcription (gray for Tn*916*, black for ICE*Bs1*). Gene names are located below the depicted open reading frame. Tn*916* gene names are abbreviated to include only the number designation from the gene name (i.e., "*orf23*" is written as "*23*"), and the corresponding ICE*Bs1* homolog gene name is written in parentheses below, when appropriate. *ardA* of Tn*916* encodes an anti-restriction protein [71]. Confirmed and putative promoters are indicated by bent arrows, putative transcription terminators in Tn*916* are indicated by "T" shapes. The current model of transcriptional regulation of Tn*916* (A) is adapted from [4]. Previously determined origins of transfer (*oriT*) and single strand origins of replication (*sso*) are indicated by a "-"above the genetic map [14,21,50,93].

https://doi.org/10.1371/journal.pgen.1009998.g001

system of ICE*Bs1* because this enables high efficiencies of element activation in donor cells and serves as the basis for regulation of hybrid elements described below.

Strains containing either ICE*Bs1* (ICE*Bs1*::*kan*), Tn*916*, or the inducible ICE*Bs1* (ICE*Bs1* Pspank-*rapI*) were grown to exponential phase in LB medium. Tn*916* and the inducible ICE*Bs1* were activated by adding either 2.5 μg/ml of tetracycline or 1mM IPTG, respectively, for one hour. We used qPCR to measure excision from the respective integration sites and normalized to a nearby chromosomal locus (*yddN* for ICE*Bs1*, and *mrpG* for Tn*916*) [14,46]. Typically, ICE*Bs1* with no exogenous activation (Table 1, row 1), Tn*916* (Table 1, row 2), and ICE*Bs1* with activation (Table 1, row 3) had excised from the chromosome in approximately 0.07%, 1–2% and ~40% of cells, respectively.

Table 1. Excision frequencies and conjugation efficiencies of ICEs.

Donor[a]	Conjugation Efficiency (%) (total donors)[b]	Donor excision frequency (%)[c]	Normalized Conjugation Efficiency (%)[d]
1. ICE*Bs1* (no external activation)	$1.2 \times 10^{-4} \pm 3 \times 10^{-5}$	0.07 ± 0.004	0.16 ± 0.03
2. Tn*916*	$1.5 \times 10^{-3} \pm 2 \times 10^{-4}$	1.5 ± 0.1	0.11 ± 0.01
3. ICE*Bs1* (*ΔrapI-phrI*)	2.7 ± 0.2	42 ± 4	6.7 ± 0.4
4. ICE*Bs1* (Δ*yddJ-yddM*)	3.2 ± 0.1	41 ± 4	8.3 ± 0.6
5. (ICE*Bs1*-Tn*916*)-H1 (Tn*916* DNA processing)	0.47 ± 0.06	41± 2	1.2 ± 0.2
6. (ICE*Bs1*-Tn*916*)-H2 (ICE*Bs1* DNA processing)	2.0 ± 0.2	42 ± 4	5.3 ± 0.4

[a] Donor strains contained the indicated ICEs: 1. JMA384 (ICE*Bs1*); 2. CMJ253 (Tn*916*); 3. JMA168 (ICE*Bs1* (Δ*rapI-phrI*); 4. ELC1211 (ICE*Bs1*{Δ(*yddJ-yddM*)}; 5. ELC1213 (H1); and 6. ELC1185 (H2). ICE*Bs1*, H1, and H2 donors (rows 3–6) contained *amyE*::[(Pspank(hy)-*rapI*) *spc*] for IPTG-inducible overproduction of RapI to de-repress the element in a large proportion of cells in the population.

[b] Donor strains were grown to exponential phase in LB medium, ICEs were stimulated with tetracycline (row 2) or IPTG (rows 3–6) for one hour, before mixing with a recipient strain (CAL419: ICE-cured, *comK*::*cat*, *str*), filtering, and placing on a solid surface for one hour. Conjugation efficiencies were calculated as the number of transconjugants (StrR and KanR for ICE*Bs1*, H1, and H2 matings; StrR and TetR for Tn*916* matings) normalized to the total number of input donors. Significant differences in conjugation efficiencies based on $P < 0.05$ in unpaired two-tailed T-tests include: Tn*916* and each of the other elements; and H1 and each of the other elements.

[c] Following element induction (rows 2–6) or without induction (row 1), DNA was harvested from an aliquot of donor cells. qPCR was used to quantify the amount of empty ICE attachment site relative to a nearby chromosomal locus (see Materials and Methods). The frequency was indicative of the percentage of donor cells in which the element had excised from the chromosome.

[d] The conjugation efficiency was divided by the excision frequency to determine the conjugation efficiency per donor with an excised element at the start of the mating. All values are the means from at least three independent mating assays. Errors are ± SEM.

https://doi.org/10.1371/journal.pgen.1009998.t001

Conjugation frequencies were measured by mixing the donor cells containing either Tn*916* or ICE*Bs1* with recipients (devoid of any conjugative element), filtering, and incubating the filters on a solid surface for one hour before selecting for transconjugants (Materials and Methods). Conjugation efficiencies of each element were calculated by normalizing the number of transconjugants to the number of total donor cells (Table 1). ICE*Bs1* with no exogenous activation, Tn*916*, and ICE*Bs1* with exogenous activation (overexpression of *rapI*) produced approximately 1.2×10^{-4}%, 1.5×10^{-3}%, and 2.7% transconjugants per donor, respectively (Table 1, rows 1–3).

Only the excised circular form of an ICE is competent for transfer. Therefore, we normalized the number of transconjugants to the excision frequency of each element. After normalization, we found that the conjugation efficiencies of ICE*Bs1* with no activation, Tn*916*, and ICE*Bs1* with activation were 0.16%, 0.11% and 6.7%, respectively, per donor with an excised element (Table 1, rows 1–3). Based on this analysis, we conclude that acquisition of ICE*Bs1* that had been activated by overexpression of *rapI* was more efficient than that of ICE*Bs1* that had not been artificially activated. The higher transfer efficiency per excision in cells overexpressing *rapI* was likely due to the irreversible de-repression of ICE*Bs1* gene expression caused by continual production of the activator RapI.

These results also indicate that acquisition of ICE*Bs1* that had been activated by overexpression of *rapI* was approximately 50-fold more efficient than that of Tn*916* that had been activated by tetracycline. This could be due to differences in any of several steps of the ICE life cycle in either donors or recipients following initial transfer of the ICE, including artificial and continuous de-repression of ICE*Bs1* gene expression due to overexpression of *rapI*, nicking, unwinding, or replication of ICE DNA, association of the ICE DNA with the conjugation machinery, DNA transfer, second strand DNA synthesis in the recipients, and integration.

Based on these considerations, we decided to build a hybrid ICE that uses the regulation, excision, and integration components of ICE*Bs1* and the DNA processing and conjugation components of Tn*916*.

Design and function of a hybrid conjugative element

Like many ICEs, both Tn*916* and ICE*Bs1* have a modular organization [47,48] with genes involved in different parts of the life cycle clustered (Fig 1). Because of this modularity, it was relatively straightforward to use the regulatory architecture of ICE*Bs1* (the genes and sequences at the left and right ends) and to replace the DNA processing and conjugation genes with those from Tn*916* (Fig 1C). Such a construct leaves intact the ICE*Bs1* genes that are required for regulation (*immA*, *immR*) and recombination (*int*, *xis*). In addition, key DNA sites are also present, including the promoter P*xis* that drives transcription of *xis* and genes downstream, and the left and right ends of the element that contain the recombination sites (*attL* and *attR*). Several genes (*yddJ*, *spbK*, and *yddM*) near the right attachment site are not required for ICE*Bs1* transfer and were omitted from the hybrid element (Fig 1C). The hybrid element, (ICE*Bs1*-Tn*916*)-H1, or H1 for short, contains a kanamycin resistance gene (*kan*) and is integrated in the genome at the normal ICE*Bs1* attachment site in *trnS-leu2* (Fig 1C).

We found that cells containing (ICE*Bs1*-Tn*916*)-H1 (ELC1213) exhibited ICE excision frequencies similar to those containing ICE*Bs1*. Cells were grown in LB medium to exponential phase. Element gene expression was induced by the addition of 1mM IPTG for one hour during exponential growth. At this time, both ICE*Bs1* and H1 had excised in ~40% of donor cells (Table 1). These results indicate that, as designed, the element H1 excises at a level similar to that of ICE*Bs1*.

Under the same mating conditions as described above, H1 produced more transconjugants/donor (0.5%) than WT Tn*916* (0.0015%), likely due to its increased activation and excision frequencies (Table 1). This is consistent with the increased conjugation efficiencies observed for Tn*916* mutants with increased excision frequencies due to mutations upstream of *tetM*, a region critical for Tn*916* regulation [49]. However, H1 consistently produced approximately 5-fold fewer transconjugants/donor than ICE*Bs1* (2.7%). This result indicates that some step(s) other than excision from the chromosome of the donor and integration into the chromosome of the transconjugant has a different efficiency than that of ICE*Bs1*.

The genes *yddJ*, *spbK*, and *yddM* from ICE*Bs1* are not present in (ICE*Bs1*-Tn*916*)-H1 and we reasoned they might contribute to the different conjugation efficiencies. We deleted these genes in ICE*Bs1* (*ΔyddJ-yddM*::*kan*) and compared excision and conjugation efficiencies relative to ICE*Bs1* (Δ*rapI-phrI*::*kan*). We found that ICE*Bs1* (*ΔyddJ-yddM*::*kan*) and ICE*Bs1* (Δ*rapI-phrI*::*kan*) behaved similarly (Table 1, rows 3, 4), indicating that there is little, if any, effect of *yddJ*, *spbK*, and *yddM* on excision or conjugation efficiencies, consistent with previous findings [36,50,51]. Together, these results indicate that steps in the ICE life cycle after excision are responsible for the differences in transfer frequencies exhibited by ICE*Bs1* (Table 1 rows 3 and 4) and (ICE*Bs1*-Tn*916*)-H1 (Table 1, row 5). In addition, because the recombinase and element ends are the same in ICE*Bs1* and H1, integration in the recipient cannot be causing the observed differences. The difference in the conjugation efficiency of each element indicates that some aspect of the conjugation functions encoded by Tn*916* are less efficient than those encoded by ICE*Bs1*.

Hybrid elements can combine different functional components required for conjugation

Following excision from the host chromosome, ICEs form circular dsDNA intermediates that are processed into a linear, ssDNA form prior to (or during) transfer to a neighboring cell [5].

First, the element-encoded relaxase (Orf20 in Tn*916*; NicK in ICE*Bs1*) nicks the DNA substrate at the origin of transfer (*oriT*) and becomes covalently attached to the 5' end of the DNA. The host-encoded translocase, PcrA, functions as a helicase to unwind the DNA, with the help of an element-encoded helicase processivity factor (Orf23 and Orf22 in Tn*916*; HelP in ICE*Bs1*) [12–14,52]. This nucleoprotein complex, termed the relaxosome, is recognized by the coupling protein (Orf21 in Tn*916*; ConQ in ICE*Bs1*) and subsequently delivered to the T4SS to be transferred to a neighboring cell [20,53–55]. The DNA processing and coupling protein components are encoded together in a module in each element (Fig 1). Because Tn*916* and ICE*Bs1* encode homologous genes required for DNA processing and conjugation, we tested if these components could be substituted between elements.

We constructed a second hybrid element that is identical to (ICE*Bs1*-Tn*916*)-H1, except it contains the DNA processing module from ICE*Bs1* in place of that from Tn*916*. This element, referred to as (ICE*Bs1*-Tn*916*)-H2, or H2, encodes the relaxase, helicase processivity factor, and coupling protein from ICE*Bs1* (Fig 1). H2 contains the single strand origin of replication from Tn*916* (*sso916*, located downstream of *orf19*) for priming second-strand synthesis during rolling-circle replication [14]. *sso1* of ICE*Bs1* was not included in H2 [21].

We found that cells containing H2 (ELC1185) had excision frequencies of ~40%, similar to those of ICE*Bs1* and H1 (Table 1). The conjugation efficiency of H2 was ~2.0% transconjugants per donor (Table 1, row 6). This is similar to the efficiencies observed for ICE*Bs1* matings, and ~4–5 fold greater than that of H1. The differences in conjugation efficiencies were not due to increased transcription of the genes in H2 relative to that in H1. We measured the amount of mRNA at the start of each mating for *orf17*, *orf16*, and *orf15* in H1 and H2 (Fig 1) using RT-qPCR and normalized to the amount of mRNA from the host gene *gyrA*. We also normalized to the amount of excision of each element. The relative amount of mRNA for *orf17*, *orf16*, and *orf15* was typically ~2-fold greater for H1 compared to H2 (9.2, 6.0, 4.2 respectively for H1 vs 4.5, 3.0, and 2.0 respectively for H2).

Together, these results indicate that the T4SS encoded by Tn*916* can support efficient conjugative transfer between *B*. *subtilis* cells and that the ICE*Bs1*-encoded coupling protein can successfully interact with the T4SS encoded by Tn*916*. They also indicate that the differences in conjugation efficiency between elements using the Tn*916* and ICE*Bs1* machineries are likely due to the relaxase, helicase processivity factor, and-or the coupling protein.

ICE*Bs1* and Tn*916* coupling proteins can substitute for each other during conjugation

The functional transfer of (ICE*Bs1*-Tn*916*)-H2 demonstrated that the ICE*Bs1* coupling protein can successfully interact with the T4SS encoded by Tn*916*. Coupling proteins must also interact with the substrate that is transferred. In this hybrid element, the coupling protein was interacting with its cognate substrate, the relaxosome (relaxase, *oriT*, and likely the helicase processivity factor) from ICE*Bs1*. In addition to transferring their own nucleoprotein complexes, both ICE*Bs1* and Tn*916* can recognize and mobilize heterologous plasmid substrates that lack their own conjugation machinery (ICE*Bs1*: pC194, pHP13, and pUB110-based pBS42; Tn*916*: pC194, pUB110, and probably others) [35,56,57]. Due to the ability to transfer similar substrates, we suspected that ICE*Bs1* and Tn*916* could transfer each other's relaxosome substrates, and that perhaps the genes encoding the coupling proteins could be substituted for one another between the elements. Therefore, we investigated the interchangeability of the coupling proteins between ICE*Bs1* and Tn*916*.

We found that the coupling proteins of Tn*916* (Orf21) and ICE*Bs1* (ConQ) can interact with their non-cognate T4SS and non-cognate relaxosome substrate. We replaced the gene

Table 2. Coupling proteins can recognize non-cognate relaxosome.

Parent Element[a]	Coupling protein gene[b]	DNA processing genes[c]	T4SS genes[c]	Conjugation Efficiency (%) (total donors)[d]	Conjugation efficiency relative to parent element[e]
1. Tn*916*	ICE*Bs1* (*conQ*)	Tn*916*	Tn*916*	0.0008 ± 0.0001	0.71 ± 0.08
2. ICE*Bs1* (*ΔrapI-phrI*)	Tn*916* (*orf21*)	ICE*Bs1*	ICE*Bs1*	0.99 ± 0.1	0.35 ± 0.03
3. H1	ICE*Bs1* (*conQ*)	Tn*916*	Tn*916*	0.25 ± 0.1	0.47 ± 0.07
4. H2	Tn*916* (*orf21*)	ICE*Bs1*	Tn*916*	1.4 ± 0.3	0.97 ± 0.2

[a] Donor strains containing the indicated ICEs had the genes encoding the coupling proteins (Orf21 for Tn*916*; ConQ for ICE*Bs1*) swapped.

[b] The indicated replacements for the gene encoding the coupling protein were made within each element: 1. Tn*916*(Δ*orf21*::*conQ*) (ELC809); 2. ICE*Bs1*(*ΔconQ*::*orf21*) (ELC866); 3. H1(Δ*orf21*::*conQ*) (ELC1584); and 4. H2(Δ*conQ*::*orf21*) (ELC1450). ICE*Bs1*, H1, and H2 donors also contained *amyE*::[(Pspank(hy)-*rapI*) *spc*] for IPTG-inducible overproduction of RapI to stimulate de-repression of element gene expression and subsequent excision.

[c] The DNA processing and T4SS genes were not changed from the parent element. For clarity, the origin of these genes is indicated here.

[d] Donor strains were grown to exponential phase in LB medium, ICE gene expression and subsequent excision was stimulated with tetracycline (row 1) or IPTG (rows 2–4) one hour before mixing with a recipient strain (CAL419: ICE-cured, *comK*::*cat str*), filtering, and placing on a solid surface for one hour. Conjugation efficiencies were calculated as the number of transconjugants (StrR and KanR for ICE*Bs1*, H1, and H2 matings; StrR and TetR for Tn*916* matings) normalized to the total number of input donors.

[e] These mating assays were conducted in parallel with the parent element (similar to the experiments from Table 1). The conjugation efficiencies of the element with the coupling protein gene swaps from (d) were normalized to the conjugation efficiencies of the parent element (with no coupling protein gene swap) in each experimental replicate to determine if there was a negative effect of using alternative coupling proteins. All values are means from three or more independent mating assays ± SEM. In all cases, the coupling protein was able to function with the heterologous element. The conjugation efficiencies were all within a factor of three, and only the comparison in row two (ICE*Bs1* with *conQ* removed and *orf20* from Tn*916* in its place, compared to ICE*Bs1*) was statistically significant ($P < 0.05$).

https://doi.org/10.1371/journal.pgen.1009998.t002

encoding the coupling protein in Tn*916*, ICE*Bs1*, (ICE*Bs1*-Tn*916*)-H1, and (ICE*Bs1*-Tn*916*)-H2 with the homologous gene (*conQ* or *orf21*) from the other element (Materials and Methods). In this way, each of these elements encoded a non-cognate coupling protein in association with the DNA processing components. Additionally, for Tn*916*, ICE*Bs1*, and (ICE*Bs1*-Tn*916*)-H1 these coupling protein replacements required interactions with the non-cognate T4SS. The H2 coupling protein swap (*conQ*::*orf21*) produced an element encoding the Tn*916* coupling protein and T4SS from Tn*916* and the DNA processing components from ICE*Bs1* (Table 2).

Cells containing an element with a coupling protein swap (ELC809, ELC866, ELC1584, and ELC1450) and cells containing the parent element were mated with recipient strain CAL419 for one hour, as described above. We found that each element containing a coupling protein swap was able to function for conjugative transfer (Table 2). The transfer frequency of Tn*916* (*orf21*::*conQ*) (ELC809) was similar to that of Tn*916* (Table 2), indicating that the coupling protein from ICE*Bs1* was able to function in the context of Tn*916* almost as well as that from Tn*916*. Similarly, ConQ was functional in the context of H1 (*orf21*::*conQ*) (ELC1584), which contains the same DNA processing and T4SS components as Tn*916*. This element mated with efficiencies ~0.25%. These results indicate that ConQ can substitute for Orf21, meaning ConQ can both recognize the relaxosome and interact with the T4SS from Tn*916*.

Orf21 also functioned in place of ConQ in ICE*Bs1* and H2 during conjugation. ICE*Bs1* (Δ*conQ*::*orf21*) (ELC866) transferred with an efficiency ~1%, averaging an approximately 3-fold decrease from ICE*Bs1* (*conQ*) matings. H2 (Δ*conQ*::*orf21*) (ELC1450) transferred with an efficiency of ~1%, which was nearly indistinguishable from that of its parent element in side-by-side comparisons.

Coupling proteins are ATPases from the HerA-FtsK superfamily of ATPases and are responsible for recognizing the transfer substrate and physically delivering it to the rest of the

conjugation machinery for export out of the cell. It is note-worthy that these coupling proteins interact with both the non-cognate transfer substrate and non-cognate conjugation machinery. Orf21 and ConQ (48% identity, 66% similarity; S1A Fig) must have enough similarity in the proper regions to enable such interactions. By analogy to other conjugation systems, the N-terminal transmembrane domains of Orf21 and ConQ likely interact with the conjugation machinery [58–62].

Previous studies determined that some coupling proteins, including TrwB of plasmid R388 and TraJ of pKM101, can interact with non-cognate conjugation machinery, but not non-cognate transfer substrates [58,59,63]. It was later determined that many conjugative coupling proteins including TrwB, VirD4 of the canonical *Agrobacterium tumefaciens* system, and PcfC of pCF10, contain a so-called "all-alpha domain" that is responsible for conferring the specificity of substrate recognition to these coupling proteins [59]. However, this domain is not present in Orf21, ConQ, and their relatives [54], and it is not yet known how these coupling proteins recognize substrates for transfer. We suspect that a conserved region of the coupling protein likely interacts with a conserved region of one or more components of the relaxosome, perhaps the relaxase. The relaxases from Tn*916* (Orf20) and ICE*Bs1* (NicK), which are 34% identical and 51% similar (S1B Fig), belong to a distinct family of conjugative relaxases and it is not yet known what translocation signal(s) they may possess [64,65].

Designing hybrid elements for transfer into *Enterococcus* species

Conjugative elements have the potential to be used as genetic tools to engineer microbes for various purposes [8–10]. However, the overall efficiency of transfer directly impacts the efficacy of this approach for genetic engineering. Although ICE*Bs1* and these ICE*Bs1*-Tn*916* hybrids can transfer with similar efficiencies from *B. subtilis* donors to *B. subtilis* recipients, we predicted that these elements might have differing abilities to interact with host machinery of different species, potentially resulting in different transfer efficiencies. For instance, Tn*916* might function more efficiently in one of its natural hosts (e.g., *Enterococcus faecalis*) than ICE*Bs1*, which is only naturally found in *B. subtilis*.

We measured the conjugation efficiency of these elements from *B. subtilis* donor cells into three different *Enterococcus* species: *E. faecalis* (the first-identified host of Tn*916*), *E. caccae*, and *E. durans*. Because *Enterococci* are naturally kanamycin resistant [66], we replaced the kanamycin resistance gene in ICE*Bs1* and the hybrid elements with *tetM* from Tn*916*. These elements are referred to as ICE*Bs1*-*tetM*, (ICE*Bs1*-Tn*916*)-H1-*tetM* (or H1-*tetM*), and (ICE*Bs1*-Tn*916*)-H2-*tetM* (or H2-*tetM*). Additionally, donor strains contained a D-alanine auxotrophy (*Δalr*::*cat*). Cells bearing this mutation will not grow on or in media without the addition of D-alanine [67], thereby serving as a mechanism for selecting against donors (counter-selecting) in a mating assay without using another antibiotic resistance gene [8].

We found that the D-alanine auxotrophy and changing the antibiotic resistance marker in ICE donors did not affect the overall conjugation efficiencies. We compared the mating efficiencies of these donors to the initial donors (*alr*+, *kan* rather than *tetM* in the elements). Donor cells containing Tn*916* (ELC1566), ICE*Bs1*-*tetM* (ELC1795), H1-*tetM* (ELC1722), or H2-*tetM* (ELC1725) were grown in LB medium containing 200 μg/ml D-alanine and mated with the *B. subtilis* recipient CAL419 under standard mating conditions as described above. Conjugation efficiencies were calculated as the number of transconjugants (tetracycline-resistant, D-alanine prototrophs) normalized to the number of donors at the start of the mating. These elements exhibited similar conjugation efficiencies as those described for the *alr*+ donors (Table 1) and are shown in Fig 2.

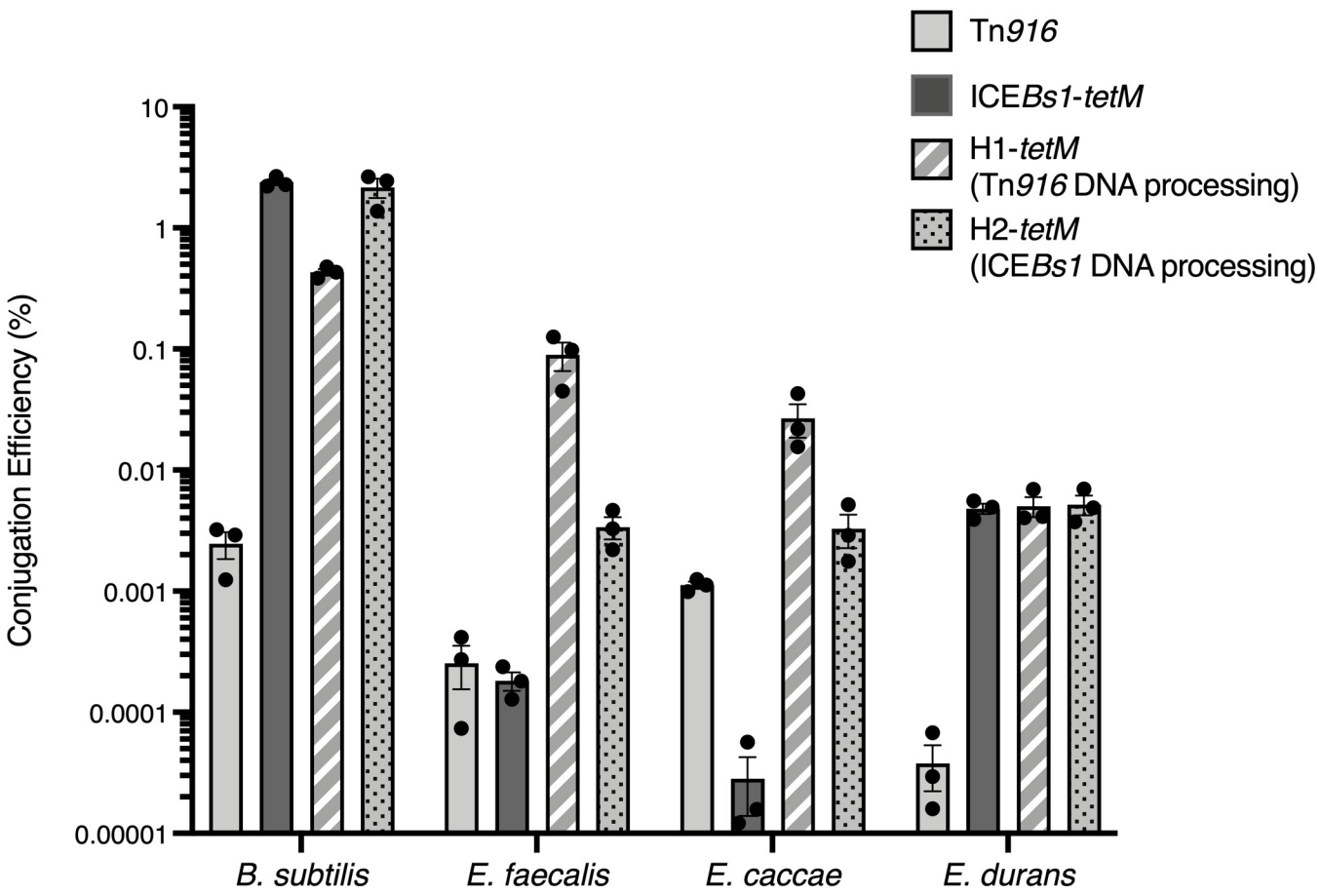

Fig 2. Element conjugation efficiencies are dependent on recipient species. *Bacillus subtilis* donors contained Tn*916* (ELC1566); ICE*Bs1* (ELC1795); (ICE*Bs1*-Tn*916*)-H1 (ELC1722); or (ICE*Bs1*-Tn*916*)-H2 (ELC1725). Donors were D-alanine auxotrophs (*alr*::*cat*) for counter-selection of transconjugants during mating assays. ICE*Bs1*, H1, and H2 donors also contained *amyE*::[(Pspank(hy)-*rapI*) *spc*] for IPTG-inducible overproduction of RapI to de-repress element gene expression that leads to excision (activation). Donor cells were grown to exponential phase in LB medium; IPTG or tetracycline was added as appropriate to stimulate element activation. Donors were mixed with recipients that had been grown to exponential phase in LB (*B. subtilis*: CAL419) or BHI (*E. faecalis*, *E. caccae*, and *E. durans*). Mixed cells were filtered and placed on a solid surface for one hour. Conjugation efficiencies were calculated as the number of transconjugants (tetR, D-alanine prototrophs) produced, normalized to the number of donors. Bars indicated the mean of 3 independent mating assays ± SEM.

https://doi.org/10.1371/journal.pgen.1009998.g002

Assessing the species specificity of transfer efficiencies

We found that the conjugation efficiencies of the various elements was dependent on the identity of the recipient species. *B. subtilis* donor cells containing Tn*916*, ICE*Bs1*-*tetM*, H1-*tetM*, or H2-*tetM*, were grown in LB medium with D-alanine, as described above. Donor cells were mixed with *E. faecalis* (ATCC 19433), *E. caccae* (BAA-1240), and *E. durans* (ATCC 6056) cells that were grown in BHI medium to exponential phase. Mixtures were filtered and placed on a solid surface for one hour for mating before resuspending cells and selecting for transconjugants that were tetracycline-resistant (ICE+) and D-alanine prototrophs (*Enterococcus*). The conjugation efficiencies were calculated as the number transconjugants produced, normalized to the number of donors applied to the mating. Aliquots of the same donor cultures were used in parallel for all comparisons with different recipients.

When these elements were mated into *E. faecalis* recipients, H1-*tetM*, which utilizes Tn*916* DNA processing and conjugation machinery, consistently produced the most transconjugants/donor (~0.09%) (Fig 2). H2-*tetM*, which is identical to H1-*tetM* except for its use of the

DNA processing module from ICE*Bs1*, produced ~0.0034% transconjugants/donor, a consistent ~30-fold decrease compared to H1-*tetM*. These consistent differences indicated that the Tn*916* DNA processing module allows for more efficient acquisition by *E. faecalis* recipients in the context of these hybrid elements. This could be due to the relaxase (encoded by *orf20*), the helicase processivity factors (encoded by *orf23* and *orf22*), and-or their interactions with host factors. Compared to the hybrid elements, ICE*Bs1* produced the fewest transconjugants per donor (0.00018%), a nearly 20-fold decrease compared to H2-*tetM*. H2-*tetM* differs from ICE*Bs1* through its use of the Tn*916* T4SS and single strand origin (*sso916*), indicating that one, or both, of these Tn*916* features contributed to more efficient acquisition by *E. faecalis*. Notably, Tn*916* produced similar numbers of transconjugants/donor as ICE*Bs1* (0.00025%). This result is in direct contrast to results observed when these elements were mated into *B. subtilis* recipients. The lower excision frequency of Tn*916* (~0.66 ± 0.08% in donors immediately prior to the start of these matings) compared to that of ICE*Bs1* (~22 ± 3%) did not correspond to lower conjugation efficiencies, indicating that steps downstream of element excision allowed for Tn*916* to produce more transconjugants.

Similar results were observed when these elements were mated into *E. caccae*, which was first isolated from human stool samples in 2006 [68]. H1-*tetM* produced the most transconjugants/donor (0.027%), which was nearly 10-fold more efficient than H2-*tetM* (0.0033%) (Fig 2). Tn*916* produced more transconjugants/donor (0.0011%) than ICE*Bs1*, which produced the fewest transconjugants of the elements tested (2.8 x 10^{-5}%). Together, these results indicate that both hybrid elements (H1-*tetM*; H2-*tetM*) are more readily acquired by *E. faecalis* and *E. caccae* than either parent element (Tn*916* and ICE*Bs1*). Notably, Tn*916* produced more transconjugants than ICE*Bs1* into these species, indicating there is a benefit to using Tn*916* genes required for conjugation. H1-*tetM* and H2-*tetM* had the advantage in that they utilize components of Tn*916* DNA processing and conjugation machinery, but the excision frequency was higher in the donor cells (~20 ± 1%, ~22 ± 8%, respectively during these experiments) than that of Tn*916* (~0.66 ± 0.08%), allowing more mating events to occur.

In contrast, the relative mating efficiencies were quite different with *E. durans* as a recipient. *E. durans* belongs to a distinct phylogenetic *Enterococcus* group (*E. faecium* group) than *E. faecalis* and *E. caccae* (*E. faecalis* group) [69]. H1-*tetM*, H2-*tetM*, and ICE*Bs1*-*tetM* all mated with similar efficiencies into *E. durans* (0.0050%, 0.0052%, and 0.0048%, respectively) (Fig 2). In contrast to the *E. faecalis* and *E. caccae* recipient matings, Tn*916* produced the fewest transconjugants/donor (3.8 x 10^{-5}%). These results indicated that Tn*916* and ICE*Bs1* DNA processing and conjugation machinery perform equally well for mating into *E. durans*, with no distinct advantage for either element. Tn*916* likely produced the fewest transconjugants due to its low excision frequency in donor cells.

Altogether, these experiments show that the identity of the recipient species impacts how efficiently a conjugative element can be acquired. Various host factors may impact how efficiently these elements can be received, including the compatibility of cell envelope structures with the conjugation machinery and the ability of these DNA elements to be processed in their new host cells upon acquisition. Furthermore, hosts may be armed to destroy newly-acquired foreign DNA with various defense systems, including restriction modification systems and CRISPR-mediated interference [1,3,70–75].

Detecting stable acquisition of conjugative elements in transconjugants

We found that ICE*Bs1* and the hybrid elements did not consistently integrate into the chromosome of the recipient cells, and thus were not stably maintained. We re-streaked transconjugants obtained from these mating assays non-selectively and subsequently checked for

tetracycline resistance. We found that fewer than 10% of the apparent transconjugants had maintained the element (S1 Table). In the few apparent transconjugants that retained tetracycline resistance, we used arbitrary PCR to map the insertion sites and frequently detected circular ICEs, indicating that the element was not stably integrated into the chromosome [8,76]. We only identified a few stable integration events in *E. caccae* and *E. durans* from H2-*tetM* matings into sites that resembled the preferred attachment site of ICE*Bs1* (S1 Table). This element went to a different location in each stable transconjugant, indicating that there is not one preferred attachment site for the element in these chromosomes. We did not identify any integration sites in *E. faecalis*. As previously reported [8], these *Enterococcus* genomes do not contain ideal ICE*Bs1* integration sites (no motifs present with >85% identity with the ICE*Bs1* 17 bp attachment site [46]). However, we have previously reported that ICE*Bs1* can integrate into sites within the *B. subtilis* chromosome containing as many as 12 mismatches from the ideal 17 bp attachment site [77].

Tn*916* was stably maintained in the transconjugants following non-selective growth. We mapped the integration sites of three transconjugants of each species and identified three unique, frequently intergenic, AT-rich integration sites in each, as expected (S1 Table) [78–80]. Because Tn*916* does not integrate in one defined chromosomal site, but instead within an AT-rich region that can be found in many places on a chromosome, Tn*916* had the advantage in target site selection and thus stable acquisition during these matings. For this reason, although Tn*916* produced fewer apparent transconjugants than H1-*tetM* or H2-*tetM*, its attachment site availability can confer an advantage during mating events. By using attachment sites from ICE*Bs1*, the hybrid element is more limited in its ability to integrate into heterologous host chromosomes.

Because the hybrid element containing Tn*916* DNA processing machinery mated more efficiently into *E. faecalis* and *E. caccae* than the hybrid containing ICE*Bs1* DNA processing machinery, we predict that the DNA processing machinery encoded by Tn*916* may be better suited for interaction with these *Enterococcus* species' host machinery. These interactions with host machinery are necessary for the element to undergo autonomous replication upon acquisition. Because ICE*Bs1* and the hybrid elements frequently did not stably integrate into these recipient chromosomes, improved replication efficiencies could improve the number of detectable transfer events. Unlike ICE*Bs1*, Tn*916* encodes two helicase processivity factors. We have not yet investigated if one or both are required to support element replication, or if these requirements change in the context of different host cells.

Summary and potential applications

Here, we showed how a hybrid element containing the easily activatable and highly efficient regulatory and integration-excision functions from ICE*Bs1* and the DNA processing and T4SS functions from Tn*916* allowed us to better define the rate-limiting steps of Tn*916* and ICE*Bs1* conjugation from *B. subtilis* hosts into various recipient species. Together, our results indicate that the host range and transfer efficiencies of conjugative elements is dictated by several different stages of the ICE life cycle.

The hybrid elements we generated demonstrate the practicality and efficiency of using the regulation and recombination (excision and integration) functions of ICE*Bs1* for studying the conjugation machinery and various functions encoded by other conjugative elements. The conjugation machinery of other elements could easily be used in place of that encoded by ICE*Bs1*, just as was the case for that from Tn*916*. The ability to induce ICE*Bs1* by overproduction of the activator RapI should allow investigation of ICEs that may be difficult to study on the population-level due to activation in a limited number of cells. Additionally, the use of

such hybrid elements might allow future host range optimization of elements for purposes of genetic engineering. It may be possible to mix and match DNA processing and conjugation machinery from different elements to be compatible with a desired recipient species. However, it is worthwhile to note that although the ICE*Bs1* DNA processing machinery and coupling protein worked with Tn*916* conjugation machinery (in H2), this will not always be the case for other hybrid elements; many elements will likely require the use of cognate transfer substrates and coupling proteins for successful transfer.

In designing future hybrid conjugative elements, it would be feasible to include genes, such as *ardA* of Tn*916* [71], to help a hybrid element defend itself against nucleolytic attack by the recipient host cell. Additionally, we imagine it would be possible to install various conjugation machines to allow transfer of different substrates, such as effector proteins, into recipient cells [81–83]. In summary, this system can be used as a chassis for future studies of Tn*916* and a variety of other conjugative elements.

Materials and methods

Media and growth conditions

B. subtilis and *Escherichia coli* cells were grown shaking at 37˚C in LB medium for all routine growth and strain constructions. *Enterococcus* cells were grown shaking at 37˚C in brain heart infusion (BHI) (Becton Dickinson, 237500) medium. When appropriate, cells were grown in liquid culture with 2.5 μg/ml kanamycin or 3 μg/ml tetracycline to maintain an ICE in donor cells (cells bearing Tn*916* were not grown in the presence of tetracycline except for periods of induction). Where indicated, donor cells containing ICE*Bs1* or a hybrid element were induced with 1mM isopropyl-β-D-thiogalactoside (IPTG) and donor cells containing Tn*916* were induced with 2.5 μg/ml tetracycline [14,22]. Cells with the D-alanine auxotrophy were grown with 200 μg/ml D-alanine. Antibiotic and other supplement concentrations for growth on solid media were: 5 μg/ml kanamycin, 12.5 μg/ml tetracycline, 100 μg/ml streptomycin, or 400 μg/ml D-alanine as appropriate.

Strains, alleles, and plasmids

E. coli strain AG1111 (MC1061 F' *lacI*^{q} *lacZM15* Tn*10*) was used for plasmid construction. *Enterococcus* strains were from the ATCC and included: *E. faecalis* ATCC-19433, *E. caccae* ATCC BAA-1240, and *E. durans* ATCC 6056.

B. subtilis strains (Table 3), except BS49, were all derived from JH642, contain the *trpC2 pheA1* alleles [84,85], and were made by natural transformation [86]. The construction of various alleles and the hybrid conjugative elements is summarized below.

ICE*Bs1* or hybrid elements were activated by overexpression of *rapI* using an isopropyl-β-D-thiogalactopyranoside (IPTG)-inducible copy of *rapI* (*amyE*::[(Pspank(hy)-*rapI) spc*]) [22]. The Δ(*rapI-phrI*)::*kan* [22] and Δ*nicK* [50] alleles in ICE*Bs1*, the Δ*orf20* [14] allele in Tn*916*, and pCAL1255 [13] were all described previously.

D-alanine auxotrophs were generated by using linearized pJAB403 to replace the open reading frames of *alrA-ndoA* (using the same borders as previously described [8]) with the chloramphenicol resistance gene from pC194.

Construction of hybrid elements

(ICE*Bs1*-Tn*916*)-H1 is a large deletion-insertion that removes the ICE*Bs1* DNA processing and conjugation genes from the start codon of *helP* through to 17 bp upstream of *yddI* and inserts Tn*916* genes from 121 bp upstream of the *orf23* start codon to the stop codon of *orf13*.

Table 3. *Bacillus subtilis* strains.

Strain	Relevant genotype[a] (reference[s])
BS49	*metB5 hisA1 thr-5 att(yufKL)*::Tn*916 att(ykyB-ykuC)*::Tn*916* [32,87,88]
JMA168	ICE*Bs1*[Δ(*rapI-phrI*)::*kan*] *amyE*::[(Pspank(hy)-*rapI*) *spc*] [22]
JMA384	ICE*Bs1*::*kan* (*kan* inserted between *yddM* and *attR*) [22]
CMJ253	*att1*::Tn*916*[b] [same as *att*(*yufKL*)::Tn*916*] [89]
CAL419	*comK*::*cat str-84* [50]
ELC809	*att1*::Tn*916*[Δ*orf21*::*conQ*]
ELC866	ICE*Bs1*[Δ*conQ*::*orf21*, Δ(*rapI-phrI*)::*kan*] *amyE*::[(Pspank(hy)-*rapI*) *spc*]
ELC1185	(ICE*Bs1*-Tn*916*)-H2 *amyE*::[(Pspank(hy)-*rapI*) *spc*]
ELC1211	ICE*Bs1*[(Δ*yddJ-yddM*)::*kan*] *amyE*::[(Pspank(hy)-*rapI*) *spc*]
ELC1213	(ICE*Bs1*-Tn*916*)-H1 *amyE*::[(Pspank(hy)-*rapI*) *spc*]
ELC1450	(ICE*Bs1*-Tn*916*)-H2[Δ*conQ*::*orf21*] *amyE*::[(Pspank(hy)-*rapI*) *spc*]
ELC1566	*att1*::Tn*916 alr*::*cat*
ELC1584	(ICE*Bs1*-Tn*916*)-H1[Δ*orf21*::*conQ*] *amyE*::[(Pspank(hy)-*rapI*) *spc*]
ELC1722	(ICE*Bs1*-Tn*916*)-H1-*tetM amyE*::[(Pspank(hy)-*rapI*) *spc*] *alr*::*cat*
ELC1725	(ICEBs1-Tn916)-H2-*tetM amyE*::[(Pspank(hy)-*rapI*) *spc*] *alr*::*cat*
ELC1795	ICEBs1[Δ(*yddJ-yddM*)::*tetM amyE*::[(Pspank(hy)-*rapI*) *spc*] *alr*::*cat*

[a] All *B. subtilis* strains, except BS49, are derived from JH642 and contain the *trpC2 pheA1* alleles (not shown) [84,85]. (ICE*Bs1*-Tn916)-H1 expanded genotype: ICE*Bs1*[Δ(*helP-yddM*)::(Tn*916*(*orf23-orf13*)) *kan*). (ICE*Bs1*-Tn*916*)-H2 expanded genotype: ICE*Bs1*[Δ(*sso1-yddM*)::(Tn*916*(*orf19-orf13*)) *kan*). Original Tn*916* gene names (*orf1-24*) are used as appropriate.

[b] *att1* is the same as *att*(*yufKL*) and maps to the region between *yufK* and *yufL* [14].

https://doi.org/10.1371/journal.pgen.1009998.t003

An additional deletion-insertion removes ICE*Bs1* genes *yddJ-yddM* starting 7 bp downstream of *yddI*'s stop codon through to the *yddM* stop codon and inserts a kanamycin resistance gene from pGK67 that is codirectional with the genes in the P*xis* operon. These fragments were fused by isothermal assembly [90] with homology arms and transformed into AG174, which contains a copy of ICE*Bs1* at *trnS-leu2*, selecting for acquisition of kanamycin resistance. ICE*Bs1* Δ*yddJ-yddM*::kan is an insertion-deletion of ICE*Bs1* identical to that contained in (ICE*Bs1*-Tn*916*)-H1.

(ICE*Bs1*-Tn*916*)-H2 is an insertion-deletion of the Tn*916* DNA processing machinery in (ICE*Bs1*-Tn*916*)-H1 removing from 121 bp upstream of the *orf23* start codon to 42 bp upstream of the *orf19* start codon and inserting ICE*Bs1* from the *helP* start codon to the *nicK* stop codon (such that this element was identical to WT ICE*Bs1* from *attL-nicK*). Two 1kb DNA fragments containing DNA flanking this region in (ICE*Bs1*-Tn*916*)-H1 were amplified and fused with the insert from ICE*Bs1* and inserted into pCAL1422, a plasmid containing *E. coli lacZ* [13], cut with BamHI and EcoRI, via isothermal assembly to generate pELC1091. The resulting plasmid was integrated by single crossover into a strain containing (ICE*Bs1*-Tn*916*)-H1. Transformants were screened for loss of *lacZ*, indicating loss of the integrated plasmid and checked by PCR for replacement of the DNA processing genes, thereby generating (ICE*Bs1*-Tn*916*)-H2. In generating this functional hybrid element, we determined the Tn*916* gene *orf19*, encoding a predicted integral membrane protein, is required for conjugative transfer.

Tetracycline-resistant variants of these ICEs were constructed by replacing *kan* with *tetM* from Tn*916*. The *tetM* insert began 274 bp upstream of *orf12* (*tetM* leader peptide) and ended with the stop codon of *tetM*. This replacement left 105 bp downstream of the *kan* ORF to serve as a transcriptional terminator. Isothermal assembly was used to fuse this replacement antibiotic cassette with ~1kb of neighboring homology regions before transforming into the

appropriate parent strain and selecting for transformants that were tetracycline resistant and confirming kanamycin sensitivity.

Δ*conQ*::*orf21* is a deletion-insertion that replaces codons 1–373 (of 480 codons) of *conQ* (ICE*Bs1*) with *orf21* (Tn*916*). The last 321 bp of *conQ* were left intact so as not to disrupt *oriT*, as previously described [56]. Δ*orf21*::*conQ* is a deletion-insertion of *orf21* (of Tn*916*), removing codons 1–424 (of 461 codons) of *orf21* and inserting the entire open reading frame of *conQ* (of ICE*Bs1*). The last 111 bp of *orf21* were left intact so as not to disrupt *oriT*. For either allele, the replacement coupling protein was fused with 1kb DNA amplifications of DNA flanking the originally encoded coupling protein and inserted into the EcoRI and BamHI cut sites of pCAL1422 by isothermal assembly. The resulting plasmids (pELC1389 and pELC801, respectively) were used to generate the deletion-insertions.

Mating assays

Mating assays were performed essentially as previously described [22]. Briefly, donor cells contained an ICE marked with either a kanamycin or tetracycline antibiotic resistance cassette. Donor cells containing either ICE*Bs1* or a hybrid element were grown in LB medium in the presence of its respective antibiotic (2.5 μg/ml kanamycin or 3 μg/ml tetracycline) to maintain ICE. Donor cells containing Tn*916* were grown non-selectively in LB medium. All donors were grown with D-alanine (200 μg/ml), as needed. *B*. *subtilis* recipient cells (CAL419) were also grown in LB medium, did not possess any ICE, were resistant to streptomycin (*str-84*), and were defective in competence (*comK*) [50]. *Enterococcus* recipient cells were grown in BHI medium and were D-alanine prototrophs.

B. *subtilis* donor strains were grown for at least three generations in LB medium to an OD_{600}~0.2 before stimulating ICE*Bs1* or Tn*916* with either 1 mM IPTG or 2.5 μg/ml tetracycline, as appropriate. After 1h, when donor and recipient cultures were at an OD_{600}~1.0, they were mixed in a 1:1 ratio (5 total ODs of cells) and applied to a nitrocellulose filter for a solid-surface mating. At this point, cells were also harvested for DNA isolation to determine via qPCR the percentage of donor cells with excised ICEs (see below). Filters were incubated on a 1.5% agar plate containing 1X Spizizen salts [86] at 37˚C for 1-3h. Cells were harvested off the filters and dilutions were plated on LB or BHI plates containing the appropriate selections to enumerate the number of transconjugants. The conjugation efficiency was calculated as the number of transconjugants present at the end of the mating (CFU/ml) divided by the number of donor cells applied to the mating (CFU/ml) (pre-mating donor counts were used to prevent an overestimation of efficiency due to a drop in viability of donor cells during the course of the mating). Where indicated, mating efficiencies were also normalized to the number of donor cells from which ICE*Bs1* or Tn*916* had excised at the start of the mating (see below).

Excision assays

We used qPCR to quantify excision of these elements. Genomic DNA of donor cultures was harvested using the Qiagen DNeasy kit with 40 μg/ml lysozyme. The following primers were used to amplify the empty ICE attachment site in the chromosome (only present in cells with excised ICE) and a nearby chromosomal locus for normalization (present in every cell).

For ICE*Bs1* and hybrid elements (integrated at *trnS-leu2*), oMA198 (5'- GCCTACTAAA CCAGCACAAC) and oMA199 (5'- AAGGTGGTTA AACCCTTGG) amplified the empty chromosomal attachment site (*attB*). oMA200 (5'- GCAAGCGATC ACATAAGGTT C) and oMA201 (5'- AGCGGAAATT GCTGCAAAG) amplified a region within the nearby gene, *yddN*.

For Tn*916* (integrated between *yufK* and *yufL*) we used previously described primers [14]. oLW542 (5'- GCAATGCGAT TAATACAACG ATAC) and oLW543 (5'- TCGAGCATTC CATCATACAT TC) amplified the empty chromosomal attachment site (*att1*). oLW544 (5'- CCTGCTTGGG ATTCTCTTTA TC) and oLW545 (5'- GTCATCTTGC ACACTTCTCT C) amplified a region within the nearby gene *mrpG*.

qPCR was performed using SSoAdvanced SYBR master mix and the CFX96 Touch Real-Time PCR system (Bio-Rad). Excision frequencies were calculated as the number of copies of the empty chromosomal attachment sites (copy numbers were determined by the standard curve method from the Cq values) [91] divided by the number of copies of the nearby chromosomal locus. Standard curves for these qPCRs were generated using *B*. *subtilis* genomic DNA that contained empty ICE attachment sites and a copy of the nearby gene (*yddN* or *mrpG*). DNA for the standard curves was harvested when these strains were in late stationary phase and had an *oriC*/*terC* ratio of ~1, indicating that the copy numbers of these targets were in ~1:1 ratios.

RT-qPCR

To measure the transcript levels of Tn*916* T4SS genes immediately prior to the start of mating, an aliquot of cells was harvested in ice-cold methanol (1:1 ratio) and pelleted. RNA was isolated using the Qiagen RNeasy PLUS kit with 10 mg/ml lysozyme. Reverse transcriptase reactions using iScript Supermix (Bio-rad) were run to generate cDNA. RNA was then degraded through the addition of 75% volume 0.1M NaOH, incubating at 70˚C for 10 minutes, and neutralizing with an equal volume of 0.1M HCl. qPCR was performed as described above. The following primers were used for amplification of the indicated site: *orf17*: oELC983 (5'–GGGAT TCCTG TGGCTTTC) and oELC984 (5'–TTGGTCGCAG TGCATAAG); *orf16*: oELC985 (5'–GCTGGGTGGT GGTAAATC) and oELC986 (5'–CCATCTGCCA CGTTCTG); *orf15*: oELC703 (5'–CTTGGACGTT CCATGACTAC) and oELC704 (5'–GAGTGATCTG CTTG TGTCC); and *gyrA*: oMEA128 (5'- TGGAGCATTA CCTTGACCAT C) and oMEA129 (5'- AGCTCTCGCT TCTGCTTTA C).

Mapping ICE integration sites

Arbitrary PCR was used to map ICE integration sites, as previously described [8,76]. Following the initial post-mating selection step, transconjugant colonies were re-streaked non-selectively onto a solid medium and subsequently checked for ICE presence by patching for tetracycline resistance. Tetracycline-resistant colonies were used as a template in a PCR reaction containing one arbitrary primer paired with an ICE-specific primer: oJ2260 (5'- GGCACGCGTC GACTAGTACN NNNNNNNNNT GATG) paired with either oJ2263 (5'- CTATTAGAAA GAAGATTAGC TGCAAACATC) for ICE*Bs1*/hybrids or oELC1009 (5'- GACATGCTAA TATAGCCATG ACG) for Tn*916*. Purified PCR products were amplified using oJ2262 (5'- G GCACGCGTC GACTAGTAC) and either oJ2265 (5'- ATCAGAACGA CCAAACAATG GT) for ICE*Bs1*/hybrids or oELC1011 (5'- GAACTATTAC GCACATGCAA C) for Tn*916*. Products were then sequenced with oJ2265 or oELC1011 and mapped to the appropriate sequenced genome. Genbank accession numbers for these species are: *B*. *subtilis* (CP007800) [85], *E*. *faecalis*, (ASDA00000000.1), *E*. *caccae* (JXKJ00000000) [92], and *E*. *durans* (ASWM01000000).

Supporting information

S1 Fig. Alignments of the coupling proteins (A) and relaxases (B) encoded by Tn*916* and ICE*Bs1*. Protein sequences were aligned with the Needleman-Wunsch algorithm (https://www.ebi.ac.uk/Tools/psa/emboss_needle/) [94]. The output alignment was shaded with

ESPript 3.0 (https://espript.ibcp.fr/ESPript/cgi-bin/ESPript.cgi) [95]. Black shading indicates identical residues; boxes indicate similar residues. A similar alignment of these relaxases has previously been reported [14].
(TIF)

S1 Table. Mapping ICE integration sites in transconjugants. This table includes information about the location and stability of different ICEs in transconjugants after transfer from specific donors. Elements and respective donors include: Tn*916* (ELC1566), ICE*Bs1*-*tetM* (ELC1795), H1-*tetM* (ELC1722), and H2-*tetM* (ELC1725).
(PDF)

Acknowledgments

We thank Jennifer Brophy for providing pJAB403 that was used to generate D-alanine auxotrophs and Monika Avello for designing primers used for excision assays.

Author Contributions

Conceptualization: Emily L. Bean, Alan D. Grossman.

Funding acquisition: Alan D. Grossman.

Investigation: Emily L. Bean, Mary E. Anderson.

Methodology: Emily L. Bean, Calvin Herman, Alan D. Grossman.

Project administration: Emily L. Bean, Alan D. Grossman.

Supervision: Alan D. Grossman.

Validation: Emily L. Bean, Calvin Herman.

Visualization: Emily L. Bean.

Writing – original draft: Emily L. Bean.

Writing – review & editing: Emily L. Bean, Calvin Herman, Mary E. Anderson, Alan D. Grossman.

References

1. Bellanger X, Payot S, Leblond-Bourget N, Guédon G. Conjugative and mobilizable genomic islands in bacteria: evolution and diversity. FEMS Microbiol Rev. 2014 Jul; 38(4):720–60. https://doi.org/10.1111/1574-6976.12058 PMID: 24372381
2. Delavat F, Miyazaki R, Carraro N, Pradervand N, van der Meer JR. The hidden life of integrative and conjugative elements. FEMS Microbiol Rev. 2017 Jul 1; 41(4):512–37. https://doi.org/10.1093/femsre/fux008 PMID: 28369623
3. Johnson CM, Grossman AD. Integrative and Conjugative Elements (ICEs): What They Do and How They Work. Annu Rev Genet. 2015; 49(1):577–601.
4. Roberts AP, Mullany P. A modular master on the move: the Tn*916* family of mobile genetic elements. Trends Microbiol. 2009 Jun; 17(6):251–8. https://doi.org/10.1016/j.tim.2009.03.002 PMID: 19464182
5. Wozniak RAF, Waldor MK. Integrative and conjugative elements: mosaic mobile genetic elements enabling dynamic lateral gene flow. Nat Rev Microbiol. 2010 Aug; 8(8):552–63. https://doi.org/10.1038/nrmicro2382 PMID: 20601965
6. Frost LS, Leplae R, Summers AO, Toussaint A. Mobile genetic elements: the agents of open source evolution. Nat Rev Microbiol. 2005 Sep; 3(9):722–32. https://doi.org/10.1038/nrmicro1235 PMID: 16138100

7. Treangen TJ, Rocha EPC. Horizontal Transfer, Not Duplication, Drives the Expansion of Protein Families in Prokaryotes. Moran NA, editor. PLoS Genet. 2011 Jan 27; 7(1):e1001284. https://doi.org/10.1371/journal.pgen.1001284 PMID: 21298028

8. Brophy JAN, Triassi AJ, Adams BL, Renberg RL, Stratis-Cullum DN, Grossman AD, et al. Engineered integrative and conjugative elements for efficient and inducible DNA transfer to undomesticated bacteria. Nat Microbiol. 2018 Sep; 3(9):1043–53. https://doi.org/10.1038/s41564-018-0216-5 PMID: 30127494

9. Miyazaki R, van der Meer JR. A New Large-DNA-Fragment Delivery System Based on Integrase Activity from an Integrative and Conjugative Element. Appl Environ Microbiol. 2013 Jul 15; 79(14):4440–7. https://doi.org/10.1128/AEM.00711-13 PMID: 23686268

10. Peters JM, Koo B-M, Patino R, Heussler GE, Hearne CC, Qu J, et al. Enabling genetic analysis of diverse bacteria with Mobile-CRISPRi. Nat Microbiol. 2019 Feb; 4(2):244–50. https://doi.org/10.1038/s41564-018-0327-z PMID: 30617347

11. Carraro N, Burrus V. The dualistic nature of integrative and conjugative elements. Mob Genet Elem. 2015 Oct 21; 5(6):98–102. https://doi.org/10.1080/2159256X.2015.1102796 PMID: 26942046

12. Lee CA, Babic A, Grossman AD. Autonomous plasmid-like replication of a conjugative transposon. Mol Microbiol. 2010 Jan 1; 75(2):268–79. https://doi.org/10.1111/j.1365-2958.2009.06985.x PMID: 19943900

13. Thomas J, Lee CA, Grossman AD. A Conserved Helicase Processivity Factor Is Needed for Conjugation and Replication of an Integrative and Conjugative Element. PLOS Genet. 2013 Jan 10; 9(1): e1003198. https://doi.org/10.1371/journal.pgen.1003198 PMID: 23326247

14. Wright LD, Grossman AD. Autonomous Replication of the Conjugative Transposon Tn*916*. J Bacteriol. 2016 Dec 15; 198(24):3355–66. https://doi.org/10.1128/JB.00639-16 PMID: 27698087

15. Carraro N, Poulin D, Burrus V. Replication and Active Partition of Integrative and Conjugative Elements (ICEs) of the SXT/R391 Family: The Line between ICEs and Conjugative Plasmids Is Getting Thinner. PLOS Genet. 2015 Jun 10; 11(6):e1005298. https://doi.org/10.1371/journal.pgen.1005298 PMID: 26061412

16. Carraro N, Libante V, Morel C, Charron-Bourgoin F, Leblond P, Guédon G. Plasmid-like replication of a minimal streptococcal integrative and conjugative element. Microbiology,. 2016; 162(4):622–32. https://doi.org/10.1099/mic.0.000219 PMID: 26825653

17. Delavat F, Moritz R, van der Meer JR. Transient Replication in Specialized Cells Favors Transfer of an Integrative and Conjugative Element. mBio. 2019 Jun 11; 10(3):e01133–19. https://doi.org/10.1128/mBio.01133-19 PMID: 31186329

18. Draper O, César CE, Machón C, Cruz F de la, Llosa M. Site-specific recombinase and integrase activities of a conjugative relaxase in recipient cells. Proc Natl Acad Sci U S A. 2005 Nov 8; 102(45):16385–90. https://doi.org/10.1073/pnas.0506081102 PMID: 16260740

19. Garcillán-Barcia MP, Jurado P, González-Pérez B, Moncalián G, Fernández LA, de la Cruz F. Conjugative transfer can be inhibited by blocking relaxase activity within recipient cells with intrabodies. Mol Microbiol. 2007 Jan 1; 63(2):404–16. https://doi.org/10.1111/j.1365-2958.2006.05523.x PMID: 17163977

20. Llosa M, Gomis-Rüth FX, Coll M, De la Cruz F. Bacterial conjugation: A two-step mechanism for DNA transport. Mol Microbiol. 2002; 45(1):1–8. https://doi.org/10.1046/j.1365-2958.2002.03014.x PMID: 12100543

21. Wright LD, Johnson CM, Grossman AD. Identification of a Single Strand Origin of Replication in the Integrative and Conjugative Element ICE*Bs1* of *Bacillus subtilis*. PLOS Genet. 2015 Oct 6; 11(10): e1005556. https://doi.org/10.1371/journal.pgen.1005556 PMID: 26440206

22. Auchtung JM, Lee CA, Monson RE, Lehman AP, Grossman AD. Regulation of a *Bacillus subtilis* mobile genetic element by intercellular signaling and the global DNA damage response. Proc Natl Acad Sci U S A. 2005 Aug 30; 102(35):12554–9. https://doi.org/10.1073/pnas.0505835102 PMID: 16105942

23. Ivins BE, Welkos SL, Knudson GB, Leblanc DJ. Transposon Tn*916* mutagenesis in *Bacillus anthracis*. Infect Immun. 1988 Jan 1; 56(1):176–81. https://doi.org/10.1128/iai.56.1.176-181.1988 PMID: 2826334

24. Franke AE, Clewell DB. Evidence for a chromosome-borne resistance transposon (Tn*916*) in *Streptococcus faecalis* that is capable of "conjugal" transfer in the absence of a conjugative plasmid. J Bacteriol. 1981 Jan; 145(1):494–502. https://doi.org/10.1128/jb.145.1.494-502.1981 PMID: 6257641

25. Franke AE, Clewell DB. Evidence for Conjugal Transfer of a *Streptococcus faecalis* Transposon (Tn*916*) from a Chromosomal Site in the Absence of Plasmid DNA. Cold Spring Harb Symp Quant Biol. 1981 Jan 1; 45:77–80. https://doi.org/10.1101/sqb.1981.045.01.014 PMID: 6271493

26. Clewell DB, Flannagan SE. The Conjugative Transposons of Gram-Positive Bacteria. In: Clewell DB, editor. Bacterial Conjugation. Boston, MA: Springer US; 1993. p. 369–93.

27. Clewell DB, An FY, White BA, Gawron-Burke C. *Streptococcus faecalis* sex pheromone (cAM373) also produced by *Staphylococcus aureus* and identification of a conjugative transposon (Tn*918*). J Bacteriol. 1985 Jun; 162(3):1212–20. https://doi.org/10.1128/jb.162.3.1212-1220.1985 PMID: 2987186

28. Fitzgerald GF, Clewell DB. A conjugative transposon (Tn*919*) in *Streptococcus sanguis*. Infect Immun. 1985 Feb; 47(2):415–20. https://doi.org/10.1128/iai.47.2.415-420.1985 PMID: 2981772

29. Roberts AP, Mullany P. Tn*916*-like genetic elements: a diverse group of modular mobile elements conferring antibiotic resistance. FEMS Microbiol Rev. 2011 Sep 1; 35(5):856–71. https://doi.org/10.1111/j.1574-6976.2011.00283.x PMID: 21658082

30. Sansevere EA, Robinson DA. Staphylococci on ICE: Overlooked agents of horizontal gene transfer. Mob Genet Elem. 2017 Aug 22; 7(4):1–10. https://doi.org/10.1080/2159256X.2017.1368433 PMID: 28932624

31. Santoro F, Vianna ME, Roberts AP. Variation on a theme; an overview of the Tn*916*/Tn*1545* family of mobile genetic elements in the oral and nasopharyngeal streptococci. Front Microbiol. 2014; 5:535. https://doi.org/10.3389/fmicb.2014.00535 PMID: 25368607

32. Christie PJ, Korman RZ, Zahler SA, Adsit JC, Dunny GM. Two conjugation systems associated with *Streptococcus faecalis* plasmid pCF10: identification of a conjugative transposon that transfers between *S. faecalis* and *Bacillus subtilis*. J Bacteriol. 1987 Jun; 169(6):2529–36. https://doi.org/10.1128/jb.169.6.2529-2536.1987 PMID: 3034859

33. Mullany P, Wilks M, Lamb I, Clayton C, Wren B, Tabaqchali S. Genetic analysis of a tetracycline resistance element from *Clostridium difficile* and its conjugal transfer to and from *Bacillus subtilis*. J Gen Microbiol. 1990 Jul; 136(7):1343–9. https://doi.org/10.1099/00221287-136-7-1343 PMID: 2172445

34. Scott JR, Kirchman PA, Caparon MG. An intermediate in transposition of the conjugative transposon Tn*916*. Proc Natl Acad Sci U S A. 1988 Jul; 85(13):4809–13. https://doi.org/10.1073/pnas.85.13.4809 PMID: 2838847

35. Naglich JG, Andrews RE. Tn*916*-dependent conjugal transfer of PC194 and PUB110 from *Bacillus subtilis* into *Bacillus thuringiensis* subsp. *israelensis*. Plasmid. 1988 Sep 1; 20(2):113–26. https://doi.org/10.1016/0147-619x(88)90014-5 PMID: 2853391

36. Avello M, Davis KP, Grossman AD. Identification, characterization and benefits of an exclusion system in an integrative and conjugative element of *Bacillus subtilis*. Mol Microbiol. 2019 Oct 1; 112(4):1066–82. https://doi.org/10.1111/mmi.14359 PMID: 31361051

37. Davis KP, Grossman AD. Specificity and selective advantage of an exclusion system in the integrative and conjugative element ICEBs1 of *Bacillus subtilis*. J Bacteriol. 2021 Mar 1; 203(10):e00700–20. https://doi.org/10.1128/JB.00700-20 PMID: 33649151

38. DeWitt T, Grossman AD. The Bifunctional Cell Wall Hydrolase CwlT Is Needed for Conjugation of the Integrative and Conjugative Element ICE*Bs1* in *Bacillus subtilis* and *B. anthracis*. J Bacteriol. 2014 Apr 15; 196(8):1588–96. https://doi.org/10.1128/JB.00012-14 PMID: 24532767

39. Celli J, Trieu-Cuot P. Circularization of Tn*916* is required for expression of the transposon-encoded transfer functions: characterization of long tetracycline-inducible transcripts reading through the attachment site. Mol Microbiol. 1998; 28(1):103–17. https://doi.org/10.1046/j.1365-2958.1998.00778.x PMID: 9593300

40. Manganelli R, Romano L, Ricci S, Zazzi M, Pozzi G. Dosage of Tn*916* Circular Intermediates in *Enterococcus faecalis*. Plasmid. 1995 Jul 1; 34(1):48–57. https://doi.org/10.1006/plas.1995.1032 PMID: 7480170

41. Scornec H, Bellanger X, Guilloteau H, Groshenry G, Merlin C. Inducibility of Tn*916* conjugative transfer in *Enterococcus faecalis* by subinhibitory concentrations of ribosome-targeting antibiotics. J Antimicrob Chemother. 2017 Oct 1; 72(10):2722–8. https://doi.org/10.1093/jac/dkx202 PMID: 29091188

42. Showsh SA, Andrews RE. Tetracycline enhances Tn*916*-mediated conjugal transfer. Plasmid. 1992 Nov; 28(3):213–24. https://doi.org/10.1016/0147-619x(92)90053-d PMID: 1334267

43. Su YA, He P, Clewell DB. Characterization of the *tet*(M) determinant of Tn*916*: evidence for regulation by transcription attenuation. Antimicrob Agents Chemother. 1992 Apr; 36(4):769–78. https://doi.org/10.1128/AAC.36.4.769 PMID: 1323953

44. Auchtung JM, Lee CA, Garrison KL, Grossman AD. Identification and characterization of the immunity repressor (ImmR) that controls the mobile genetic element ICE*Bs1* of *Bacillus subtilis*. Mol Microbiol. 2007; 64(6):1515–28. https://doi.org/10.1111/j.1365-2958.2007.05748.x PMID: 17511812

45. Jones JM, Grinberg I, Eldar A, Grossman AD. A mobile genetic element increases bacterial host fitness by manipulating development. eLife. 2021 Mar 3; 10:e65924. https://doi.org/10.7554/eLife.65924 PMID: 33655883

46. Lee CA, Auchtung JM, Monson RE, Grossman AD. Identification and characterization of *int* (integrase), *xis* (excisionase) and chromosomal attachment sites of the integrative and conjugative element ICE*Bs1*

of *Bacillus subtilis*. Mol Microbiol. 2007 Dec 1; 66(6):1356–69. https://doi.org/10.1111/j.1365-2958.2007.06000.x PMID: 18005101

47. Burrus V, Waldor MK. Shaping bacterial genomes with integrative and conjugative elements. Res Microbiol. 2004 Jun; 155(5):376–86. https://doi.org/10.1016/j.resmic.2004.01.012 PMID: 15207870

48. Toussaint A, Merlin C. Mobile Elements as a Combination of Functional Modules. Plasmid. 2002 Jan; 47(1):26–35. https://doi.org/10.1006/plas.2001.1552 PMID: 11798283

49. Beabout K, Hammerstrom TG, Wang TT, Bhatty M, Christie PJ, Saxer G, et al. Rampant Parasexuality Evolves in a Hospital Pathogen during Antibiotic Selection. Mol Biol Evol. 2015 Oct 1; 32(10):2585–97. https://doi.org/10.1093/molbev/msv133 PMID: 26060280

50. Lee CA, Grossman AD. Identification of the Origin of Transfer (*oriT*) and DNA Relaxase Required for Conjugation of the Integrative and Conjugative Element ICE*Bs1* of *Bacillus subtilis*. J Bacteriol. 2007 Oct 15; 189(20):7254–61. https://doi.org/10.1128/JB.00932-07 PMID: 17693500

51. Johnson CM, Harden MM, Grossman AD. Interactions between mobile genetic elements: An anti-phage gene in an integrative and conjugative element protects host cells from predation by a temperate bacteriophage. PLOS Genet. 2022 Feb 14; 18(2):e1010065. https://doi.org/10.1371/journal.pgen.1010065 PMID: 35157704

52. Auchtung JM, Aleksanyan N, Bulku A, Berkmen MB. Biology of ICE*Bs1*, an integrative and conjugative element in *Bacillus subtilis*. Plasmid. 2016 Jul 1; 86:14–25. https://doi.org/10.1016/j.plasmid.2016.07.001 PMID: 27381852

53. Alvarez-Martinez CE, Christie PJ. Biological Diversity of Prokaryotic Type IV Secretion Systems. Microbiol Mol Biol Rev MMBR. 2009 Dec; 73(4):775–808. https://doi.org/10.1128/MMBR.00023-09 PMID: 19946141

54. Iyer LM, Makarova KS, Koonin EV, Aravind L. Comparative genomics of the FtsK–HerA superfamily of pumping ATPases: implications for the origins of chromosome segregation, cell division and viral capsid packaging. Nucleic Acids Res. 2004 Jan 1; 32(17):5260–79. https://doi.org/10.1093/nar/gkh828 PMID: 15466593

55. Schröder G, Lanka E. The mating pair formation system of conjugative plasmids—A versatile secretion machinery for transfer of proteins and DNA. Plasmid. 2005 Jul 1; 54(1):1–25. https://doi.org/10.1016/j.plasmid.2005.02.001 PMID: 15907535

56. Lee CA, Thomas J, Grossman AD. The *Bacillus subtilis* Conjugative Transposon ICE*Bs1* Mobilizes Plasmids Lacking Dedicated Mobilization Functions. J Bacteriol. 2012 Jun; 194(12):3165–72. https://doi.org/10.1128/JB.00301-12 PMID: 22505685

57. Showsh SA, Andrews RE. Analysis of the Requirement for a pUB110 *mob* Region during Tn*916*-Dependent Mobilization. Plasmid. 1999 May 1; 41(3):179–86. https://doi.org/10.1006/plas.1999.1398 PMID: 10366523

58. Llosa M, Zunzunegui S, Cruz F de la. Conjugative coupling proteins interact with cognate and heterologous VirB10-like proteins while exhibiting specificity for cognate relaxosomes. Proc Natl Acad Sci. 2003 Sep 2; 100(18):10465–70. https://doi.org/10.1073/pnas.1830264100 PMID: 12925737

59. Whitaker N, Chen Y, Jakubowski SJ, Sarkar MK, Li F, Christie PJ. The All-Alpha Domains of Coupling Proteins from the *Agrobacterium tumefaciens* VirB/VirD4 and *Enterococcus faecalis* pCF10-Encoded Type IV Secretion Systems Confer Specificity to Binding of Cognate DNA Substrates. J Bacteriol. 2015 Jul 15; 197(14):2335–49. https://doi.org/10.1128/JB.00189-15 PMID: 25939830

60. Segura RL, Águila-Arcos S, Ugarte-Uribe B, Vecino AJ, de la Cruz F, Goñi FM, et al. The transmembrane domain of the T4SS coupling protein TrwB and its role in protein–protein interactions. Biochim Biophys Acta. 2013 Sep 1; 1828(9):2015–25. https://doi.org/10.1016/j.bbamem.2013.05.022 PMID: 23735543

61. Álvarez-Rodríguez I, Ugarte-Uribe B, de la Arada I, Arrondo JLR, Garbisu C, Alkorta I. Conjugative Coupling Proteins and the Role of Their Domains in Conjugation, Secondary Structure and in vivo Subcellular Location. Front Mol Biosci. 2020; 7:185. https://doi.org/10.3389/fmolb.2020.00185 PMID: 32850972

62. Steen JA, Bannam TL, Teng WL, Devenish RJ, Rood JI. The Putative Coupling Protein TcpA Interacts with Other pCW3-Encoded Proteins To Form an Essential Part of the Conjugation Complex. J Bacteriol. 2009 May; 191(9):2926–33. https://doi.org/10.1128/JB.00032-09 PMID: 19251842

63. Hamilton CM, Lee H, Li P-L, Cook DM, Piper KR, von Bodman SB, et al. TraG from RP4 and TraG and VirD4 from Ti Plasmids Confer Relaxosome Specificity to the Conjugal Transfer System of pTiC58. J Bacteriol. 2000 Mar; 182(6):1541–8. https://doi.org/10.1128/JB.182.6.1541-1548.2000 PMID: 10692358

64. Wawrzyniak P, Płucienniczak G, Bartosik D. The Different Faces of Rolling-Circle Replication and Its Multifunctional Initiator Proteins. Front Microbiol. 2017; 8:2353. https://doi.org/10.3389/fmicb.2017.02353 PMID: 29250047

65. Garcillán-Barcia MP, Francia MV, De La Cruz F. The diversity of conjugative relaxases and its application in plasmid classification. FEMS Microbiol Rev. 2009 May 1; 33(3):657–87. https://doi.org/10.1111/j.1574-6976.2009.00168.x PMID: 19396961

66. Murray BE. The Life and Times of the Enterococcus. Clin Microbiol Rev. 1990 Jan; 3(1):46–65. https://doi.org/10.1128/CMR.3.1.46 PMID: 2404568

67. Wecke J, Madela K, Fischer W. The absence of D-alanine from lipoteichoic acid and wall teichoic acid alters surface charge, enhances autolysis and increases susceptibility to methicillin in *Bacillus subtilis*. Microbiology. 1997 Sep 1; 143(9):2953–60. https://doi.org/10.1099/00221287-143-9-2953 PMID: 33657735

68. Carvalho M da GS, Shewmaker PL, Steigerwalt AG, Morey RE, Sampson AJ, Joyce K, et al. *Enterococcus caccae* sp. nov., isolated from human stools. Int J Syst Evol Microbiol. 2006 Jul 1; 56(7):1505–8.

69. Byappanahalli MN, Nevers MB, Korajkic A, Staley ZR, Harwood VJ. Enterococci in the Environment. Microbiol Mol Biol Rev MMBR. 2012 Dec; 76(4):685–706. https://doi.org/10.1128/MMBR.00023-12 PMID: 23204362

70. Cury J, Oliveira PH, de la Cruz F, Rocha EPC. Host Range and Genetic Plasticity Explain the Coexistence of Integrative and Extrachromosomal Mobile Genetic Elements. Mol Biol Evol. 2018 Sep; 35(9):2230–9. https://doi.org/10.1093/molbev/msy123 PMID: 29905872

71. Serfiotis-Mitsa D, Roberts GA, Cooper LP, White JH, Nutley M, Cooper A, et al. The Orf18 Gene Product from Conjugative Transposon Tn*916* Is an ArdA Antirestriction Protein that Inhibits Type I DNA Restriction–Modification Systems. J Mol Biol. 2008 Nov; 383(5):970–81. https://doi.org/10.1016/j.jmb.2008.06.005 PMID: 18838147

72. Tock MR, Dryden DT. The biology of restriction and anti-restriction. Curr Opin Microbiol. 2005 Aug; 8(4):466–72. https://doi.org/10.1016/j.mib.2005.06.003 PMID: 15979932

73. Westra ER, Swarts DC, Staals RHJ, Jore MM, Brouns SJJ, van der Oost J. The CRISPRs, they are a-changin': how prokaryotes generate adaptive immunity. Annu Rev Genet. 2012; 46:311–39. https://doi.org/10.1146/annurev-genet-110711-155447 PMID: 23145983

74. Wilson GG, Murray NE. Restriction and modification systems. Annu Rev Genet. 1991 Dec 1; 25(1):585–627.

75. Zhang Q, Rho M, Tang H, Doak TG, Ye Y. CRISPR-Cas systems target a diverse collection of invasive mobile genetic elements in human microbiomes. Genome Biol. 2013 Apr 29; 14(4):R40. https://doi.org/10.1186/gb-2013-14-4-r40 PMID: 23628424

76. Das S, Noe JC, Paik S, Kitten T. An improved arbitrary primed PCR method for rapid characterization of transposon insertion sites. J Microbiol Methods. 2005 Oct 1; 63(1):89–94. https://doi.org/10.1016/j.mimet.2005.02.011 PMID: 16157212

77. Menard KL, Grossman AD. Selective Pressures to Maintain Attachment Site Specificity of Integrative and Conjugative Elements. PLOS Genet. 2013 Jul 18; 9(7):e1003623. https://doi.org/10.1371/journal.pgen.1003623 PMID: 23874222

78. Cookson AL, Noel S, Hussein H, Perry R, Sang C, Moon CD, et al. Transposition of Tn*916* in the four replicons of the *Butyrivibrio proteoclasticus* B316(T) genome. FEMS Microbiol Lett. 2011 Mar; 316(2):144–51. https://doi.org/10.1111/j.1574-6968.2010.02204.x PMID: 21204937

79. Mullany P, Williams R, Langridge GC, Turner DJ, Whalan R, Clayton C, et al. Behavior and Target Site Selection of Conjugative Transposon Tn*916* in Two Different Strains of Toxigenic *Clostridium difficile*. Appl Environ Microbiol. 2012 Apr 1; 78(7):2147–53. https://doi.org/10.1128/AEM.06193-11 PMID: 22267673

80. Scott JR, Bringel F, Marra D, Alstine GV, Rudy CK. Conjugative transposition of Tn*916*: preferred targets and evidence for conjugative transfer of a single strand and for a double-stranded circular intermediate. Mol Microbiol. 1994; 11(6):1099–108. https://doi.org/10.1111/j.1365-2958.1994.tb00386.x PMID: 8022279

81. Bhatty M, Laverde Gomez JA, Christie PJ. The expanding bacterial type IV secretion lexicon. Res Microbiol. 2013 Jul 1; 164(6):620–39. https://doi.org/10.1016/j.resmic.2013.03.012 PMID: 23542405

82. Segal G, Purcell M, Shuman HA. Host cell killing and bacterial conjugation require overlapping sets of genes within a 22-kb region of the *Legionella pneumophila genome*. Proc Natl Acad Sci U S A. 1998 Feb 17; 95(4):1669–74. https://doi.org/10.1073/pnas.95.4.1669 PMID: 9465074

83. Souza DP, Oka GU, Alvarez-Martinez CE, Bisson-Filho AW, Dunger G, Hobeika L, et al. Bacterial killing via a type IV secretion system. Nat Commun. 2015 May; 6(1):6453.

84. Perego M, Spiegelman GB, Hoch JA. Structure of the gene for the transition state regulator, *abrB*: regulator synthesis is controlled by the *spo0A* sporulation gene in *Bacillus subtilis*. Mol Microbiol. 1988; 2(6):689–99. https://doi.org/10.1111/j.1365-2958.1988.tb00079.x PMID: 3145384

85. Smith JL, Goldberg JM, Grossman AD. Complete Genome Sequences of *Bacillus subtilis* subsp. *subtilis* Laboratory Strains JH642 (AG174) and AG1839. Genome Announc. 2014 Jul 3; 2(4):e00663–14. https://doi.org/10.1128/genomeA.00663-14 PMID: 24994804

86. Harwood CR, Cutting SM. Molecular biological methods for *Bacillus*. Chichester, United Kingdom: John Wiley & Sons; 1990. 581 p.

87. Browne HP, Anvar SY, Frank J, Lawley TD, Roberts AP, Smits WK. Complete genome sequence of BS49 and draft genome sequence of BS34A, *Bacillus subtilis* strains carrying Tn*916*. FEMS Microbiol Lett. 2015 Feb 1; 362(3):1–4. https://doi.org/10.1093/femsle/fnu050 PMID: 25673660

88. Haraldsen JD, Sonenshein AL. Efficient sporulation in *Clostridium difficile* requires disruption of the σK gene. Mol Microbiol. 2003; 48(3):811–21. https://doi.org/10.1046/j.1365-2958.2003.03471.x PMID: 12694623

89. Johnson CM, Grossman AD. Identification of host genes that affect acquisition of an integrative and conjugative element in *Bacillus subtilis*. Mol Microbiol. 2014 Sep 1; 93(6):1284–301. https://doi.org/10.1111/mmi.12736 PMID: 25069588

90. Gibson DG, Young L, Chuang R-Y, Venter JC, Hutchison CA, Smith HO. Enzymatic assembly of DNA molecules up to several hundred kilobases. Nat Methods. 2009 May; 6(5):343–5. https://doi.org/10.1038/nmeth.1318 PMID: 19363495

91. Bustin SA, Nolan T. Data analysis and interpretation. In: A-Z of quantitative PCR. La Jolla, CA: International University Line; 2004. p. 439–92.

92. Zhong Z, Zhang W, Song Y, Liu W, Xu H, Xi X, et al. Comparative genomic analysis of the genus *Enterococcus*. Microbiol Res. 2017 Mar 1; 196:95–105. https://doi.org/10.1016/j.micres.2016.12.009 PMID: 28164795

93. Jaworski DD, Clewell DB. A Functional Origin of Transfer (*oriT*) on the Conjugative Transposon Tn*916*. J Bacteriol. 1995; 177:6644–51. https://doi.org/10.1128/jb.177.22.6644-6651.1995 PMID: 7592445

94. Madeira F, Park YM, Lee J, Buso N, Gur T, Madhusoodanan N, et al. The EMBL-EBI search and sequence analysis tools APIs in 2019. Nucleic Acids Res. 2019 Jul 1; 47(W1):W636–41. https://doi.org/10.1093/nar/gkz268 PMID: 30976793

95. Robert X, Gouet P. Deciphering key features in protein structures with the new ENDscript server. Nucleic Acids Res. 2014 Jul 1; 42(W1):W320–4. https://doi.org/10.1093/nar/gku316 PMID: 24753421